

Brillouin-Scattering Measurements from Plasmas Irradiated with Spatially and Temporally Incoherent Laser Light

A. N. Mostovych, S. P. Obenschain, J. H. Gardner,^(a) J. Grun, K. J. Kearney, C. K. Manka, E. A. McLean, and C. J. Pawley^(b)

Laser Plasma Branch, Plasma Physics Division, Naval Research Laboratory, Washington, D.C. 20375

(Received 27 April 1987)

Stimulated Brillouin-scattering spectra have been measured from plasmas produced by spatially and temporally incoherent laser light. The measured backscatter spectra and intensities differ substantially from measurements of Brillouin scattering with coherent illumination. Backscatter is strongly suppressed and the Brillouin signature in the spectra disappears. This quenching of stimulated Brillouin scattering is observed even when the laser coherence time is much larger ($10\times$) than the predicted convective saturation time of the stimulated-Brillouin-scattering instability.

PACS numbers: 52.25.Rv

The excitation of parametric instabilities depends on a coherent feedback process between a strong pump wave and the resultant decay waves. Any process which interferes with the coherence of the feedback mechanism can alter the behavior of the instability. Control of parametric instabilities is an important requirement for the success of laser-produced fusion. For example, if too high a laser intensity is used, stimulated Brillouin scattering (SBS) may be an important loss mechanism.¹

In this Letter we present the first measurements of SBS from a plasma that is produced by spatially and temporally incoherent laser beams. We find that SBS is strongly suppressed by the combination of temporal and spatial incoherence. These results are not adequately explained by the current theory of parametric instabilities.

Temporal incoherence is generated by use of a broadband laser oscillator. The broadband pulse has both random phase and amplitude modulation. To obtain spatial incoherence we use the induced spatial incoherence (ISI)

technique.^{2,3} ISI introduces rapidly changing (laser-coherence time scale) spatial nonuniformities in the focused laser profile. On time scales much longer than the laser coherence time these nonuniformities average out to produce uniform illumination. A schematic of the experimental setup is shown in Fig. 1. A 2-nsec-duration Nd-doped-glass laser beam (1.054 or $0.527\ \mu\text{m}$) is reflected by two sets of ISI echelons and focused with a 2-m lens onto a planar CH target. Each echelon assembly consists of about 25 strip mirrors stacked in a stepwise fashion. The two assemblies are oriented perpendicular to each other and the step size between the reflecting surfaces (2 psec for the first assembly and 40 psec for the second) is larger than the typical coherence time (1 psec) of the broadband oscillator. The cumulative reflection from both echelons produces a beam composed of many statistically independent rectangular beamlets. These beamlets overlap incoherently in the focal plane to produce a very uniform time-averaged il-

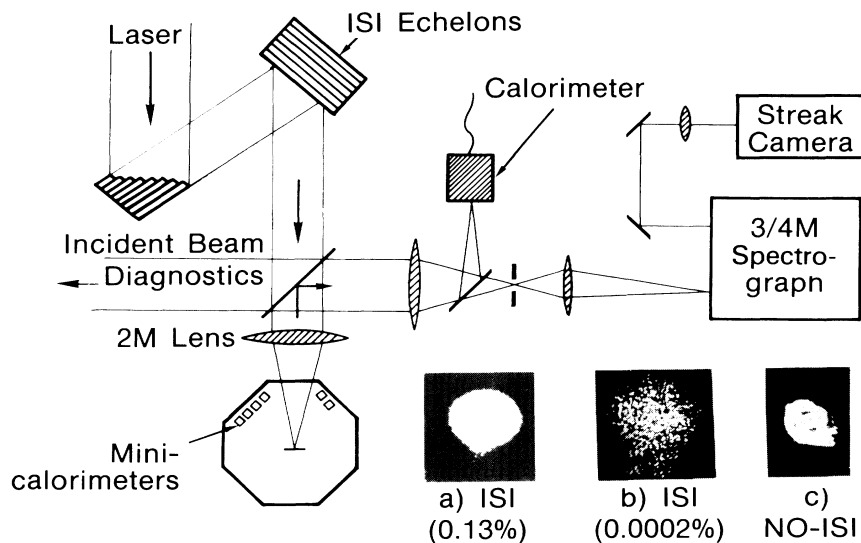


FIG. 1. Schematic of the experiment used to study SBS with ISI illumination. Typical focal-spot distributions are included: (a) echelons with broad bandwidth (0.13%), (b) echelons with narrow bandwidth (time-bandwidth limit), and (c) standard beam, i.e., no echelons.

lumination profile. The degree of smoothing with respect to the average laser intensity is proportional to the root coherence-to-averaging time ratio, $\Delta I/I \approx (\tau_c/\tau_a)^{1/2}$.

To determine the effects of temporal incoherence, spatial incoherence, and amplitude modulation separately, data were taken with and without the ISI echelons for various laser bandwidths ($\Delta\omega/\omega = 0.3\%$, $\tau_c \approx 0.6$ psec; and 0.03% , 6 psec for $\lambda = 0.527 \mu\text{m}$; $\Delta\omega/\omega = 0.13\%$, $\tau_c \approx 2.7$ psec; 0.06% , 5.9 psec; 0.01% , 35 psec; and 0.0002% , 1750 psec for $\lambda = 1.054 \mu\text{m}$). With the echelons and the broadest bandwidths, the time-averaged focal spot on target is very smooth, $\Delta I/I \leq 5\%$ [Fig. 1(a)]. For the narrowest bandwidth, the time-bandwidth limit $\Delta\nu = 1/\tau$ (0.0002%), of the 2-nsec laser pulse, the laser coherence length is much longer than the echelon steps. The overlapped beamlets interfere coherently and a very spiky focal distribution [Fig. 1(b)] is produced. The combination of narrow bandwidth and echelons produces even higher peak intensities than are found in a standard (nonechelon) beam [Fig. 1(c)]. The average intensities (within the FWHM for ISI and the 90% energy contour for non-ISI) were the same for the different cases. Finally, in the time-bandwidth limit there are no amplitude modulations in the output of a laser.

The observed SBS is predominantly confined to backscatter through the lens (Fig. 2). For the case with ISI echelons and medium to broad laser bandwidth ($\Delta\omega/\omega \geq 0.3\%$ at $0.527 \mu\text{m}$ and 0.01% at $1.054 \mu\text{m}$) the

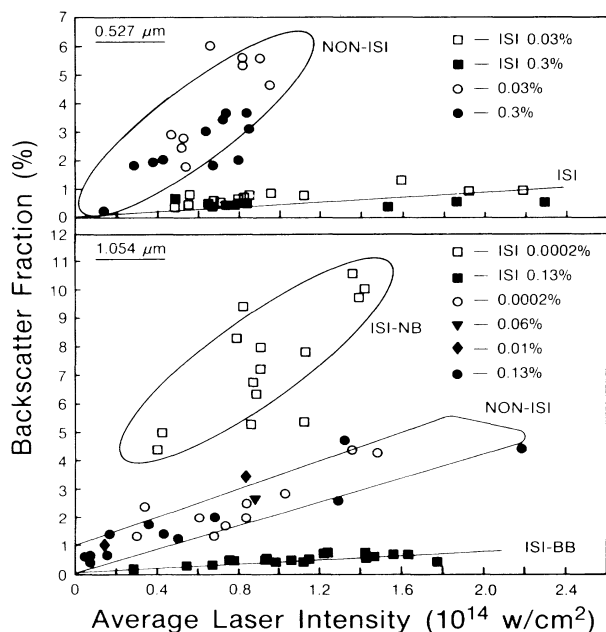


FIG. 2. SBS backscatter fraction as a function of average laser intensity. Without the ISI echelons, bandwidth has no significant effect on the backscatter. With the echelons in place the backscatter is strongly suppressed for broad-bandwidth ($\Delta\omega/\omega \geq 0.01\%$) laser beams (ISI-BB) while for very narrow bandwidths (0.0002%) (ISI-NB) it is increased.

SBS backscatter is reduced by as much as an order of magnitude relative to a standard echelon-free beam [Fig. 1(c)]. Conversely, for the time-bandwidth limit (0.0002%) with echelons, the SBS backscatter fraction is practically double that of the standard echelon-free beam. Figure 3 plots some of the same data versus peak intensity instead of average intensity. The backscatter of the ISI beam is still substantially lower than for the echelon-free shots. Therefore, the effectiveness of ISI in suppressing the SBS instability is greater than would be expected from simple intensity averaging of the laser hot spots. Note also that the broad-bandwidth (0.13%) and narrow-bandwidth (0.0002%) echelon cases have similar peak instantaneous focal intensities but the backscatter is strongly suppressed with broad bandwidth. One explanation for this is that the growth time of the instability is longer than the laser coherence time and SBS sees the smooth profile. It may also be possible that the density modulations produced by the broadband ISI generate incoherence which suppress the instability.

Without the echelons in place, there is no significant effect on the amount of backscatter even when the laser bandwidth is varied between 0.0002% and 0.3% . Theoretical work^{4,5} predicts that bandwidth will not be important unless $\gamma/\Delta\omega \ll 1$, where γ is the homogeneous growth rate. This is consistent with the data since $\gamma/\Delta\omega$ is of order 1 or larger in our work.

Even though the backscatter fraction does not depend on the bandwidth, time-resolved measurements reveal a temporal structure in the backscattered light which is sensitive to bandwidth. Typical streak-camera photographs of the backscattered light at $\lambda = 1.054 \mu\text{m}$ are shown in Figs. 4(a)-4(c) for the 0.13% , 0.01% , and 0.0002% bandwidths (without echelons). There is sub-

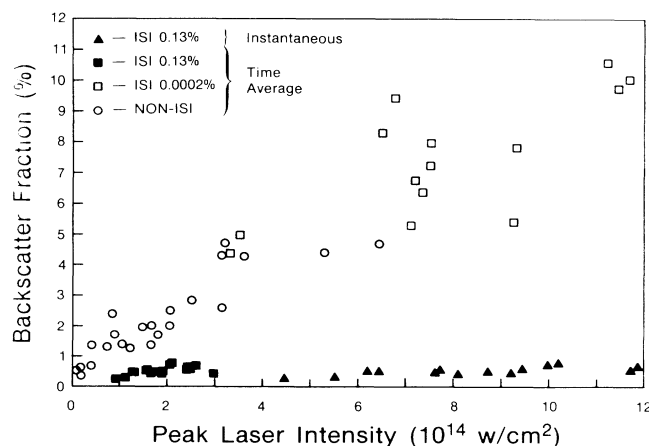


FIG. 3. Backscatter as a function of peak time-averaged laser intensity. The ISI backscatter is lower even though the peak intensities are the same as for the non-ISI case. Also, ISI backscatter with broad bandwidth is much lower than the narrow-band case irrespective of the fact that the peak instantaneous intensities are the same.

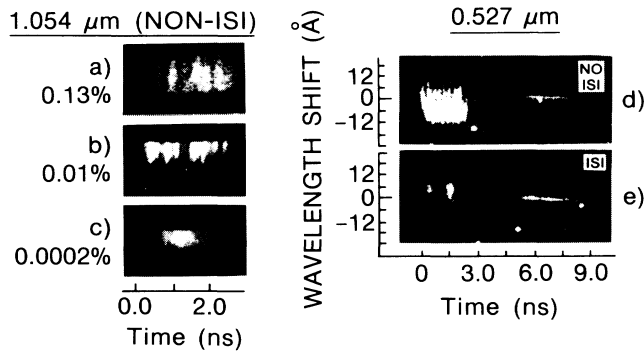


FIG. 4. Streak-camera photographs of the backscattered light. The 1.054- μm data show the bandwidth-dependent modulation of the spectrally integrated backscatter. The 0.527- μm data contrast the temporal and spectral behavior of the backscatter (first signal) and delayed incident light (late signal) for the cases with and without the ISI echelons for $\Delta\omega/\omega=0.03\%$.

stantial modulation of the backscatter for the $\Delta\omega/\omega=0.01\%$ and 0.13% cases, but no modulation occurs for the time-bandwidth-limited 0.0002% case. These modulations are believed to be caused by the incident laser which exhibits similar temporal structure. For the 0.527- μm case the backscattered spectra as well as the incident light intensity are time resolved. The echelon-free backscatter spectra are consistently strongly shifted to the blue during the laser pulse while the ISI backscatter spectra are neutral or slightly shifted to the red. Strong time modulations are visible in the intermediate-bandwidth (0.03%) echelon-free data whereas with echelons the time evolution of the spectra is relatively smooth. The absence of time modulations in the ISI spectra, even at the intermediate bandwidth, probably reflects some averaging process due to the ISI echelons or possibly quenching of SBS by ISI.

The time-integrated 0.527- μm spectra (Fig. 5) show the same large blue shift (4–5 Å) for non-ISI data and a basically neutral shift (± 1 Å) for the ISI case. These shifts occur for both the 0.3% and 0.03% bandwidths and they progress toward the blue with increased laser intensity. Both the 0.527- and 1.054- μm spectra exhibit linewidths which are larger than the wavelength shifts and are much broader ($1.5\times-5\times$) than the incident laser linewidth.

If we use the dispersion relations for ion-acoustic waves, the SBS k -matching conditions, and a 2D hydrodynamic calculation of the local plasma conditions, we find that the blue-shifted 0.527- μm non-ISI spectra originate near one-quarter to one-half critical density where the plasma flow is supersonic. The neutral or slightly red-shifted ISI spectra come from the subsonic regions close to the critical surface. For the 1.054- μm data, the plasma flow is supersonic all the way up to the critical surface and the spectra appear to originate close to the critical surface [(0.6–1) n_c]. There is no observable

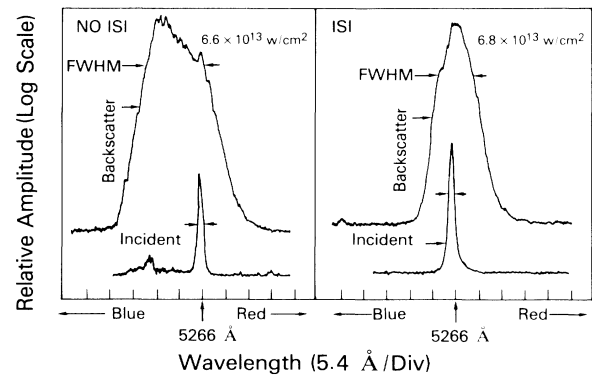


FIG. 5. Sample time-integrated backscatter spectra for the narrower-bandwidth 0.527- μm case. Without ISI the spectra are strongly shifted to the blue. This corresponds to SBS in the underdense plasma where the plasma flow is supersonic. With ISI the blue shift is replaced with little or no shift.

change in the wavelength shift for the 1.054- μm data with or without the ISI echelons. This difference between the two wavelengths may be explained by the very different regions of strong SBS gain.

The point of maximum SBS gain occurs where the laser intensity, plasma density, and plasma scale lengths are maximized. At 0.527- μm , this occurs in the (0.25–0.5) n_c region and coincides with the origin of the blue-shifted non-ISI spectra. Since the blue-shifted spectra are correlated with regions of strong SBS gain and disappear with ISI, it follows that ISI quenches the SBS instability to below the detection threshold. (The very weak unshifted ISI spectra may simply be due to residual reflections from the critical surface.) At 1.054 μm , however, collisional absorption is much less effective and the laser intensity remains high (above 50% versus a few percent at 0.527 μm) all the way up to the critical surface. As a result, the SBS gain, which increases with density, has a strong gain region all the way to the critical surface. At $\lambda=1.054$ μm the SBS origination and reflection points now nearly coincide, thereby accounting for the lack of a wavelength shift between the ISI and non-ISI data at 1.054 μm .

It is difficult to explain the measured ISI results with the theory of the SBS instability in inhomogeneous plasmas.^{6–8} The standard theoretical models of SBS in an inhomogeneous plasma are based on either the slowly varying envelope ($kC_s \gg \gamma$) or the quasimode approximation ($kC_s \ll \gamma$). In this experiment, γ is of order kC_s . Calculations based on the quasimode model⁷ predict only about one e -folding of growth before saturation; if this were true we would see no backscatter in any of the experiments. On the other hand, in the slow-wave approximation, the total convective SBS gain in an inhomogeneous plasma is given by $\exp(2\pi\gamma^2/K'V_1V_2)$, where γ is the homogeneous growth rate, K' is the phase-mismatch wave number, and V_1 and V_2 are the ion-acoustic and

scattered-light wave group velocities. The instability grows from the point of perfect phase matching with the homogeneous growth rate until the growth envelope has convected out of the phase-matching region—at which time ($t \approx 4\gamma/K'V_1V_2$) the growth saturates at the value given above. Applying this model to our 2D hydrodynamic simulations ($T_e \approx 900$ eV, $V \approx 4 \times 10^7$ cm/sec, $L_r \approx 200$ μm : at $\frac{1}{4}n_c$) of the 0.527- μm experiment, we find that between $0.1n_c$ and $0.5n_c$, where the gain is maximum, the homogeneous growth rate is on the order of 3.5×10^{12} sec^{-1} ; the convective saturation time is about 1 psec, and the number of intensity e -foldings is about seven.

If the saturation time (1 psec) of the instability is indeed shorter than a single laser coherence time then spatial averaging with ISI echelons should not be important. But we find that the ISI echelons are effective in quenching the SBS instability even when the laser coherence time is as long as 10 psec. Apparently the slow-wave approximation overestimates the gain of the instability when the homogeneous growth rate is comparable to the ion-acoustic frequency.⁹ As a result, the instability may grow over more laser coherence times and is therefore susceptible to the spatial incoherence generated by the ISI echelons.

The role of filamentation for our experimental conditions was examined by numerical calculations.¹⁰ The calculations indicate that filamentation is unlikely to occur at 0.527 μm for $I < 10^{14}$ W/cm^2 while being very likely at 1.054 μm . The fact that ISI suppresses SBS for both wavelengths suggests that filamentation alone cannot explain the behavior of SBS in this experiment.

In conclusion, measurements of spectral and time-resolved SBS have been obtained with and without ISI echelons and with broad and narrow bandwidths. SBS

backscatter is strongly suppressed by ISI. Present theory is not adequate to explain these findings because the slow-wave approximation is not valid for this experiment.

We wish to acknowledge useful discussions with S. E. Bodner, R. H. Lehmberg, B. H. Ripin, A. J. Schmitt, and J. A. Stamper. We thank L. Daniels, J. Ford, N. Nocerino, and M. Pronko for their assistance during the course of this experiment. This research was supported by the U.S. Department of Energy.

^(a)Present address: Laboratory for Computational Physics, Naval Research Laboratory, Washington, D.C. 20375.

^(b)Present address: Science Applications International Corp., McLean, VA 22102.

¹B. H. Ripin, F. C. Young, J. A. Stamper, C. M. Armstrong, R. Decoste, E. A. McLean, and S. E. Bodner, *Phys. Rev. Lett.* **39**, 611 (1977).

²S. P. Obenschain, J. Grun, M. J. Herbst, K. J. Kearney, C. K. Manka, E. A. McLean, A. N. Mostovych, J. A. Stamper, R. R. Whitlock, S. E. Bodner, J. H. Gardner, and R. H. Lehmberg, *Phys. Rev. Lett.* **56**, 2807 (1986).

³R. H. Lehmberg and S. P. Obenschain, *Opt. Commun.* **46**, 27 (1983).

⁴J. J. Thomson, W. K. Kruer, S. E. Bodner, and J. S. DeGroot, *Phys. Fluids* **17**, 849 (1974).

⁵J. J. Thomson, *Nucl. Fusion* **15**, 237 (1975).

⁶M. N. Rosenbluth, R. B. White, and C. S. Liu, *Phys. Rev. Lett.* **31**, 1190 (1973).

⁷C. S. Liu, M. N. Rosenbluth, and R. B. White, *Phys. Fluids* **17**, 1211 (1974).

⁸D. W. Forslund, J. M. Kindel, and E. L. Lindman, *Phys. Fluids* **18**, 1002 (1975).

⁹J. F. Drake *et al.*, *Phys. Fluids* **17**, 778 (1974).

¹⁰A. J. Schmitt, to be published.

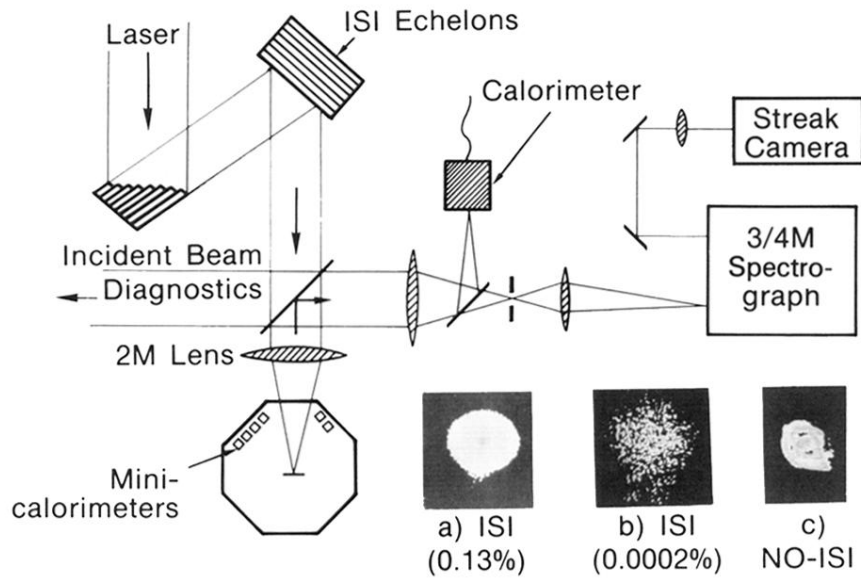


FIG. 1. Schematic of the experiment used to study SBS with ISI illumination. Typical focal-spot distributions are included: (a) echelons with broad bandwidth (0.13%), (b) echelons with narrow bandwidth (time-bandwidth limit), and (c) standard beam, i.e., no echelons.

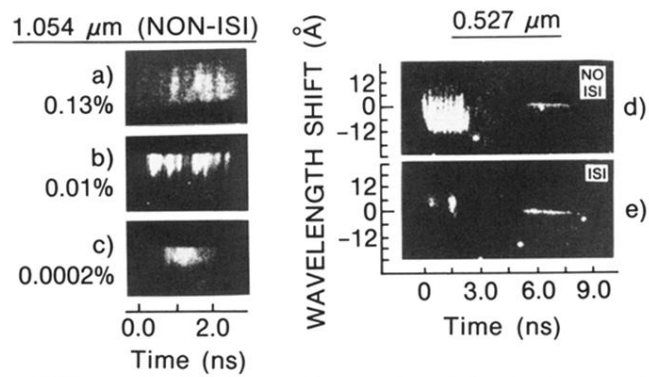


FIG. 4. Streak-camera photographs of the backscattered light. The 1.054- μm data show the bandwidth-dependent modulation of the spectrally integrated backscatter. The 0.527- μm data contrast the temporal and spectral behavior of the backscatter (first signal) and delayed incident light (late signal) for the cases with and without the ISI echelons for $\Delta\omega/\omega=0.03\%$.